

Dependence of the flux-creep activation energy on the magnetization current for a $\text{La}_{1.86}\text{Sr}_{0.14}\text{CuO}_4$ single crystal

M. E. McHenry, S. Simizu, and H. Lessure

Department of Metallurgical Engineering and Materials Science, Carnegie Mellon University, Pittsburgh, Pennsylvania 15213

M. P. Maley and J. Y. Coulter

Los Alamos National Laboratory, Los Alamos, New Mexico 87545

I. Tanaka and H. Kojima

Institute of Inorganic Synthesis, Yamanashi University, Kofu 400, Japan

(Received 14 March 1991)

Magnetic relaxation and hysteresis studies have been performed for a *c*-axis-oriented single crystal of $\text{La}_{1.86}\text{Sr}_{0.14}\text{CuO}_4$. We demonstrate that the effective activation energy for flux creep, U_{eff} , is a strongly nonlinear function of the current density J (as given by the irreversible magnetization). For fixed fields of 0.5, 1.0, 2.0, and 3.0 T and temperatures between 4 and 15 K (as consistent with full field penetration of the sample), $U_{\text{eff}}(J)$ is seen to vary approximately logarithmically with J . A scaling relationship, $U_{\text{eff}}(J) = [-U_1 g(T)/H^n] \ln(J/J_c)$, is shown to be obeyed for this crystal with $n \approx 0.9$ (H in T), $U_1 \approx 180 k_B$, and $J_c(1 \text{ T}) \approx 3.2 \times 10^5 \text{ A/cm}^2$. Several functional forms of $g(T)$ have been explored and shown to give reasonable fits if monotonically decreasing in temperature over the range where flux creep is observed. We also explore the ramifications of this functional dependence in explaining an observed exponential temperature dependence of the hysterically determined critical current density. Finally, we show that comparison of the temperature dependence of logarithmic relaxation rate $A = dM/d \ln(t)$ and the derivative of the magnetization with respect to $\ln(T)$ at fixed time, $dM_0/d \ln(T)$, can be used to set a scale of the attempt frequency for flux motion consistent with the other measurements.

INTRODUCTION

Magnetic relaxation,¹⁻⁴ thermally activated resistance,⁵ flux noise,⁶ and ac magnetic response⁷ of high-temperature superconductors have all been interpreted by appealing to an Arrhenius rate equation:

$$v = v_0 \exp \left[\frac{-U_{\text{eff}}}{kT} \right], \quad (1)$$

where v represents the rate of flux hopping, v_0 is an attempt frequency, and U_{eff} is an effective energy barrier to flux motion. Only for nearly spatially invariant flux distributions and therefore small currents does the effective barrier energy approximate the true volume pinning energy of the material. For other experiments where significant shielding or transport currents are present, the pinning energy is reduced by an energy which can be associated with the Lorentz force density multiplied by a suitably correlated volume and hop distance. Flux-creep measurements are experiments which probe a tilted energy barrier or so-called "washboard" potential for fluxons.⁸

Beasley *et al.*⁸ have treated the problem of a nonlinear magnetic diffusion equation for the case of a diffusion coefficient which depends on B and ∇B . A one-dimensional version of the flux conservation relationship proposed by Beasley can be expressed as

$$\frac{dB}{dt} = \nabla \cdot \left[Ba v_0 \exp \left[\frac{-U_{\text{eff}}}{kT} \right] \right], \quad (2)$$

where B is the local flux density and a the hop distance for fluxons or flux bundles. To express the rate of change of the average flux density $\langle B \rangle$, expression (2) is integrated over the sample volume. Considering a slab geometry (of thickness d) and using the divergence theorem results in the following expression for the rate of change of average flux density in the sample:

$$\frac{d\langle B \rangle}{dt} = 4\pi \frac{dM}{dt} = \frac{2Ha v_0}{d} \exp \left[\frac{U_{\text{eff}}(j_s, H)}{kT} \right], \quad (3)$$

here the effective energy is taken to be a function of flux density and the gradient of flux density, where the boundary condition requires their evaluation at the interface. In the analysis of flux-creep data it has been customary to assume that the effective barrier energy is related linearly to the current density:

$$U_{\text{eff}} = U_0 - JBVa, \quad (4)$$

where V represents the correlation volume. The proportionality of the magnetization and the current density J allows for the expression

$$\frac{dM}{dt} \approx \frac{dJ}{dt} \approx \exp \left[\frac{-JBVa}{kT} \right], \quad (5)$$

which can be solved to reveal a logarithmic time dependence for J or equivalently M .

It is typical in creep measurements to use the slope of magnetization versus $\ln(t)$ to infer information as to the value of the average volume pinning potential. The analysis of Beasley *et al.*⁸ has shown that the rate of change of the current density per logarithmic increment of time can be expressed in terms of the derivative of the effective pinning potential with respect to current density. Expressed equivalently in terms of the magnetization, this relationship is

$$A = \frac{dM}{d \ln(t)} = kT \left[\frac{\partial U_{\text{eff}}}{\partial M} \right]^{-1}. \quad (6)$$

Exploiting a linear relationship between U_{eff} and J or alternatively M as given by (4) results in a relationship from which the volume pinning energy U_0 can be inferred from measurement of the logarithmic magnetic relaxation rate:

$$\frac{1}{M_0} \frac{dM}{d \ln(t)} = \left[\frac{-kT}{U_0} \right]. \quad (7)$$

Here M_0 is the magnetization prior to the beginning of the relaxation process (or that corresponding to the unrelaxed value of the critical current density). This formalism has been commonly used to extract pinning energies from magnetic relaxation data for many high-temperature superconducting materials. However, it should be pointed out that the formalism applies only for the linear $U_{\text{eff}}(J)$ relationship (4) and to logarithmic creep.

In a recent study by Maley *et al.*⁹ it has been shown that an analysis of magnetic relaxation data appealing directly to the rate equation (3) for thermally activated flux motion, rather than logarithmic time fits of $M(t)$ data, offered an attractive means of extracting the explicit magnetization and therefore J dependence of the effective flux-creep potential, U_{eff} . Further, it was determined for c -axis-oriented (grain-aligned) Y-1:2:3 that this effective potential was nonlinear in J , approximately obeying a $\ln(J)$ dependence consistent with earlier observations by Zeldov *et al.*¹⁰ based on transport measurements. This observation of a nonlinear potential serves to clarify several important anomalies resulting from a previous analysis of creep data in which a linear approximation (4) was used. These anomalies include the following.

- (1) A large disparity in U_0 as determined from magnetic relaxation and transport measurements.^{1,5}
- (2) An increasing apparent activation energy as a function of temperature.^{11,12}
- (3) With increasing temperature an increasing time range both at short and long times where a $\ln(t)$ fit of $M(t)$ is inadequate. This extends to the regime where the diffusion constant for flux motion becomes unvarying with field and current and solution of the diffusion equation yields an exponential time dependence.¹³

Given the possibility of a strong nonlinear relationship between the effective potential and the current density, only expression (6) rigorously holds for logarithmic relaxation data and the use of (7) to analyze magnetic relaxa-

tion data leads to an apparent activation energy¹¹ where the above-mentioned anomalies may apply. If an analysis based on the rate equation itself is used, it appears that the functional dependence U_{eff} on J can be unambiguously determined from magnetization versus time data. It is our purpose here to investigate the latter procedure more fully to interpret magnetic relaxation data for a high-quality $\text{La}_{1.86}\text{Sr}_{0.14}\text{CuO}_4$ single crystal. Specifically, we examine the field dependence of $U_{\text{eff}}(J)$ and examine the extent to which a $\ln(J)$ or other nonlinear dependence adequately describes these energy functionals at different fields. Secondly, we explore the manifestation of such a nonlinear dependence on the temperature dependence of the hysteretically derived current density, J . We will refer to the volume average current density as J and the critical current density as J_c . The hysteretically determined value, J , is distinguished from the critical current density, J_c , from which the hysteretic value has crept away (note that this is different from the designations J_c and J_{c0} used in Ref. 1 but equivalent to that used in Ref. 8). Finally, we will show that similarities in the temperature dependence of the logarithmic magnetic relaxation rate $A = dM/[d \ln(t)]$ and the derivative of the magnetization with respect to the logarithm of temperature at fixed time $dM_0/[d \ln(T)]$, can also be understood within this framework of the flux-creep model and gives further evidence of its validity.

EXPERIMENTAL DETAILS

All experiments reported here have been performed on a $\text{La}_{1.86}\text{Sr}_{0.14}\text{CuO}_4$ (La-Sr-Cu-O) single crystal with fields oriented along the c axis. The sample was prepared using a traveling solvent floating-zone technique.¹⁴ The crystal was aligned along the tetragonal (room-temperature) cell principal axes and polished so that the faces were parallel to within 1° . The polished sample had dimensions of $2.890 \times 2.816 \times 2.405 \text{ mm}^3$ all $\pm 0.01 \text{ mm}$ with the shortest axis being the c axis. The density was measured to be 6.882 g/cm^3 consistent with the nominal Sr content. This particular crystal is the same as used in recent studies of the temperature dependence of elastic constants above the tetragonal to orthorhombic phase transition.¹⁵

Magnetic measurements were performed on a Quantum Design SQUID magnetometer operating with a 3-cm scan length to minimize field inhomogeneity effects. When corrected for demagnetization, the crystal exhibited full shielding diamagnetism at 4 K an $H = 10 \text{ G}$. An onset temperature for superconductivity of 36 K was observed in a field of 20 G. A hysteretic current density of $2.4 \times 10^5 \text{ A/cm}^2$, in zero field and 5 K, has been calculated using the Bean model for a cylindrical geometry where the cylinder radius is taken as the geometric mean of the sides of the parallelepiped which are orthogonal to the field direction (i.e., in the ab plane). This current density is more than an order of magnitude smaller than that observed in typical c -axis Y-1:2:3 crystals and nearly 2 orders of magnitude smaller than that observed in neutron-irradiated single crystals with enhanced pinning.¹⁶ The weak pinning in this crystal is perhaps indicative of its degree perfection and absence of defects. In light of this

weak pinning, the magnetic irreversibility line, as shown in Fig. 1, is very shallow extending to lower temperatures at relatively small fields (i.e., ~ 5 T at 5 K). This irreversibility line is somewhat arbitrarily determined from the point at which magnetic hysteresis curves (taken over ~ 2 – 3 h periods) are observed to pinch off and that hysteresis is no longer discernible (to ~ 0.01 emu resolution). This serves as an approximate irreversibility line and serves as one of the experimental boundaries for magnetic relaxation measurements. Due to the shallow nature of the irreversibility line, studies of magnetic relaxation at small reduced temperatures, $< \sim 0.4T_c$, are limited to a narrow field range. Figure 1 also shows the temperature dependence of the full penetration field (i.e., the field at which flux entirely penetrates the sample volume). In the Bean and critical state models for magnetic hysteresis this can be taken to be roughly the field at which the peak in the $M(H)$ curve occurs. We restrict our magnetic relaxation experiments to fields between the full penetration field and the irreversibility line. For fields beyond the full penetration field, as examined here, demagnetization corrections are relatively small and are therefore ignored. All magnetic relaxation measurements were made by first starting in the zero-field-cooled state and then applying a field (using the SQUID no overshoot mode) so as to begin the magnetic decay on the virgin magnetization curve. The duration of these relaxation measurements was typically 2–3 h.

RESULTS AND DISCUSSION

Figure 2 illustrates the dependence of the effective activation energy as a function of magnetization for applied fields of 0.5, 1.0, 2.0, and 3.0 T, respectively. The nonlinear $U_{\text{eff}}(J)$ potential is determined using an analysis which appeals directly to the rate equation (3). Following

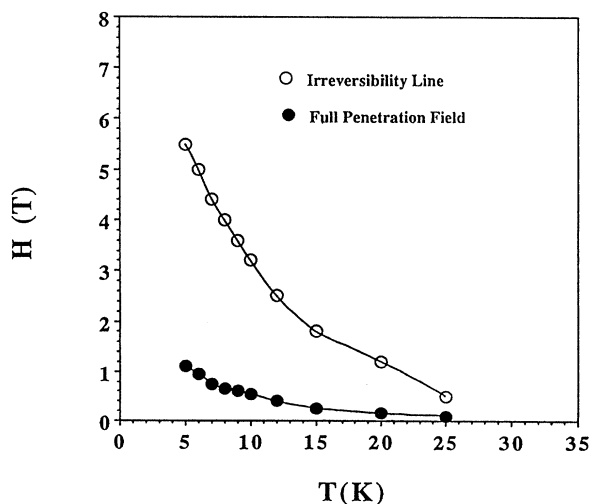


FIG. 1. Magnetic irreversibility line $H^{\text{irr}}(T)$ and full penetration field $H^*(T)$ as determined from magnetic hysteresis measurements.

Ref. 9 and rearranging expression (3),

$$\frac{U_{\text{eff}}}{k} = -T \left[\ln \left| \frac{dM(t)}{dt} \right| - \ln \left[\frac{H \nu_0 a}{2\pi d} \right] \right] \quad (8)$$

yields the algorithm for obtaining the effective pinning potential from $M(t)$ data recognizing that the argument of the second logarithm is essentially constant for fixed field and $T \ll T_c$. The rate equation derived in the Beasley analysis pertains to relaxation at fields greater than those required for full penetration of the sample, thus the data shown in Fig. 2 is restricted to temperatures (at a given field) large enough to ensure complete flux penetration of the sample and in all cases less than $\sim 0.4T_c$ (exclusion of the curve corresponding to the largest U_{eff} in each data set restricts the data to less than $\sim 0.3T_c$). $U_{\text{eff}}(J)$ curves are constructed from magnetization versus time data at fixed field and temperatures between 4 and 15 K. Each set of points, at a fixed field, reflects a magnetic relaxation measurement made at a different temperature. Analysis of the time derivative of the magnetization and corresponding value of M (both at a fixed time) allows for fitting of the data in the form suggested by (8). Values of the constant, $C = \ln[(H \nu_0 a)/2\pi d]$ were determined to be 36, 27, 24, and 23 for the fields of 0.5, 1.0, 2.0, and 3.0 T. Note that these values were determined by the requirement of continuity of the $U_{\text{eff}}(J)$ curve as determined by eye and therefore are good only to approximately ± 2 . Several notable features of the $U_{\text{eff}}(J)$ dependence are evident from the figure.

(1) Data have been taken over temperature intervals ($\Delta T \sim 1$ K) so that relaxation data at increasing temperatures and fixed fields are shown to overlap on several of

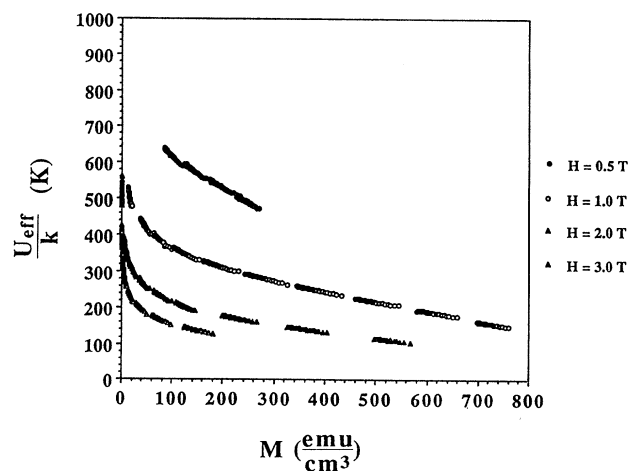


FIG. 2. $U_{\text{eff}}(J)$ as determined from measurements of the time-dependent magnetic relaxation $M(t, T)$, using expression (8), for fixed fields of 0.5, 1.0, 2.0, and 3.0 T, respectively. Data at 0.5 T is constructed from relaxation measurements at temperatures between 10 and 15 K, respectively; that at 1.0, 2.0, and 3.0 T is from 5 to 15 K. Values of the constant $C = \ln(H \nu_0 a / 2\pi d)$ used for these fits were 36, 27, 24, and 23 for the fields of 0.5, 1.0, 2.0, and 3.0 T, respectively.

the $U_{\text{eff}}(J)$ versus J plots. The choice of a single additive constant at each field is seen to yield a continuous $U_{\text{eff}}(J)$ which is shown to shift to increasing energies with decreasing fields. The quality of this fit is seen to deteriorate to some degree for the data sets taken at the highest temperatures (lowest values of M). For these fits, the constant $C = \ln[(H\nu_0 a)/2\pi d]$, is determined to be a strongly changing function of applied field H . Given that C can be related to parameters which should display only weak field variation and which appear as arguments of a logarithm, we view this as an unphysical variation. It will be further shown that both the failure of the fits at higher temperatures and the unphysical variation of C on H is an artifact which can be removed by suitable temperature scaling of the effective barrier energy. The unreasonable field dependence of the constant is reflective of the fact that the curves at lower fields are fit using $M(t)$ data sets at progressively higher temperatures (so as to be consistent with the full penetration requirement). This data is then more apt to show problems associated with inevitable temperature scaling of the effective activation energy barrier associated with the temperature dependence of the correlated volume for flux motion and the hop distance. It will be seen that the relatively invariant value of C as a function of applied field is obtained by fitting only very low-temperature data. The high-temperature data can then be fit only after a suitable scaling with temperature.

(2) All relaxation data at a given field begin at nearly equivalent values of U_{eff}/kT . This was also observed previously in grain-aligned Y-1:2:3 materials.⁹ This value is designated $(U_{\text{eff}}/kT)_0$ and represents the value determined at the first measured magnetization points in an $M(t)$ sequence occurring a nearly constant time of ~ 360 sec. This starting value is seen to be reflection of the value of the attempt frequency ν_0 and the fixed experimental time $\tau \sim 360$ sec. Values of $(U_{\text{eff}}/kT)_0$ are seen to vary in much the same way as the constant C does on the applied field.

(3) As in the prior study of grain-aligned Y-1:2:3, the effective activation energy at each field is seen to be nonlinear in J and appears to follow a $\ln(J)$ dependence over the limited range studied. Much higher effective activation energies are observed at low values of M (or equivalently J). One possible way of viewing this behavior is by appealing to a distribution of activation energy barriers so that, at low values of J , the still pinned flux is associated with the strongest barriers, the flux in the weakest barriers having already been overcome at typical experimental starting times. However, a similar response can also be predicted¹⁰ by appealing to atomistic models to explain a strongly nonlinear dependence of the energy barrier height on the current density. In this instance, U_{eff} is larger at lower J due to reduction of the Lorentz force related energy which reduces the bias towards forward (into the sample) flux motion.

Although the data fits shown in Fig. 2 give a reasonable description of the $U_{\text{eff}}(J)$ dependence, there are still several issues which remain troubling. These include the fact that the highest-temperature data is not as well fit as

the low-temperature data. More important is the fact that, although the fixed field data is seen to follow a single universal curve using a single value of the constant C , this constant required to fit flux-creep data at different values of the applied field is seen to vary in an unphysical way as a function of this field. Certainly, this variation of C , between 23 and 36, and its apparent implication that the argument of $\ln[(H\nu_0 a)/2\pi d]$ varies over many orders of magnitude is unsatisfying. One explanation for the disparity in the values of the constant C required to fit the flux-creep data to the form suggested by expression (8) is the fact that the absolute energy scale for flux motion must also reflect the scaling of fundamental pinning related parameters on temperature and field. Tinkham¹⁷ has examined just such scaling laws in the high-temperature regime in order to explain flux-creep-induced broadening of the resistive transition in an applied field. In this analysis, the Ginzburg-Landau temperature dependences of the condensation energy, as well as of pinning related length scales (i.e., the coherence length and fluxon lattice spacing) were considered and a $(1-t)^{3/2}/B$ scaling of the effective activation energy for thermally activated flux motion (U_{eff}/kT) was inferred for temperatures near T_c . This Ginzburg-Landau treatment also does, in fact, predict a much flatter temperature dependence at low temperatures ($\sim 1-t^2$). We have also considered possible temperature scalings of the effective energy, U_{eff} for low-temperature thermally activated flux motion. Surprisingly, we have found that a similar $g(t) = (1-t)^{3/2}$ temperature scaling ($t = T/T_c$), as shown in Fig. 3(a), also allows for the smooth variation of U_{eff} with M (and equivalently J) but also with the same value of the additive constant ($C = 19$). Such a scaling then offers the appeal of allowing for fitting with a single constant C for all fields examined but with a slope of the scaling function at low temperatures that disagrees with that predicted by the Ginzburg-Landau theory arguments. Notice that this scaling approach differs from a more ad hoc approach of assuming that the constant C itself is strongly temperature dependent.

Further scrutiny of this temperature dependence reveals that it is basically the monotonically decreasing nature of $g(t)$ over the temperature range in which the flux creep has been examined which allows for the fitting with a single constant at the various field values. The $(1-t)^{3/2}$ temperature scaling is not consistent with the flat temperature dependence of Ginzburg-Landau derived parameters at low temperatures. However, a $1-t^2$ dependence, as suggested by Tinkham as the low-temperature scaling behavior, does not serve to remove the disparity in the values of the additive constant C . This has led us to consider yet another plausible temperature scaling in which the low-temperature Ginzburg Landau (GL) form is utilized, but instead of the reduced temperature scale being determined by T_c it is instead assumed to be scaled by the field-dependent irreversibility line temperature T^* . Our procedure then is to rely on a flat temperature dependence at low temperatures for the scaling function and thus determine the constant C by using only low-temperature $M(t)$ data and fitting the higher-temperature

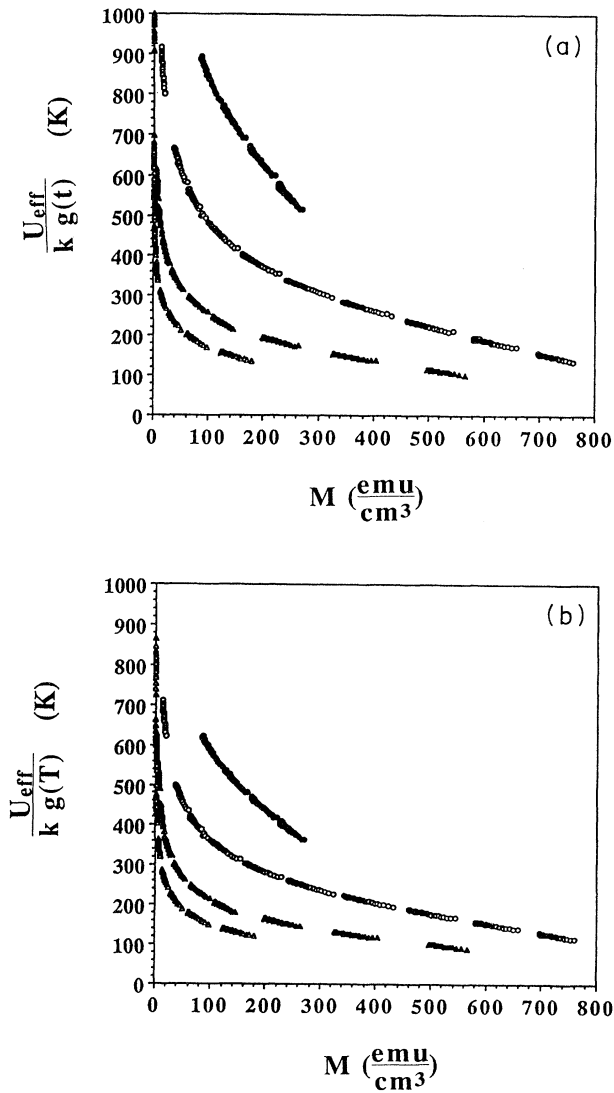


FIG. 3. (a) Fits of $[U_{\text{eff}}(J)/g(t)]$ vs M for fixed fields of 0.5, 1.0, 2.0, and 3.0 T, respectively. Here $g(t) = (1-t)^{3/2}$. (b) Similar fits of $[U_{\text{eff}}(J)/g(T)]$ vs M for fixed fields of 0.5, 1.0, 2.0, and 3.0 T, respectively. Here $g(T) = 1 - (T/T_{\text{irr}})^2$ where T_{irr} has been treated as a fitting parameter and determined to be 25, 22, 19, and 16 K for the respective fields between 0.5 and 3.0 T.

data using a scaling function of temperature which also has zero slope at $T = 0$ K. We thus examine in Fig. 3(b) the scaling of the U_{eff} data with the function $g(T) = 1 - (T/T_{\text{irr}})^2$ where T_{irr} is taken as a fitting parameter which is determined to be 25, 22, 19, and 16 K for the 0.5-, 1.0-, 2.0-, and 3.0-T data, respectively. It can be seen that these values are in reasonable agreement with both the magnitude and field dependence of the irreversibility line. It can also be seen that fits of similar quality to $U_{\text{eff}}(J)$, again with a single value of the constant C ($C = 19$), is possible with this scaling. Fitting with this $g(T)$ then offers a more realistic curvature at low temperatures, though at the expense requiring an ad-

ditional fitting parameter (T_{irr}). The success of this fit may be taken to imply that the irreversibility line does indeed determine the scale of the effective activation energy.

Theoretical support for a $g(T)$ that exhibits a substantial slope extending to $T < T_c/2$ in contrast to the GL prescriptions is provided by treatments based upon the collective pinning model^{18,19} that derives a "thermal smearing" mechanism whereby thermal vibrations of the vortex lattice (VL) averaged over the collective pinning potential and cause a steep reduction in U_{eff} near the VL melting temperature. Recent experimental determinations, by Palstra *et al.*,²⁰ of activation energies from transport measurements on Bi and Tl compounds also show a steep decrease beginning at low temperatures ($T/T_c < 0.2$) and scaled by a temperature $T_x \approx T_c/2$. This rapid depression of U_{eff} at temperatures $\ll T_c$ is strongly correlated with the anisotropy of the HTS compound. Our present analysis is not capable of determining the details of $U_{\text{eff}}(T)$, but, clearly, a more rapid decrease at low temperature than is provided by the GL expressions, with T_c as the scaling temperature, is required to yield a consistent fit to the data.

In both Figs. 3(a) and 3(b), the scaling of the U_{eff} data by monotonically decreasing functions of temperature were shown to both improve the quality of the fits of $U_{\text{eff}}(J)$ at high temperatures and to provide more reasonable values of the constant ($C = \ln[(Hv_0a)/2\pi d] \sim 19$). This constant is now seen to be relatively invariant with field which we believe to be physically more realistic. Although $(1-t)^n$ power laws have been used to fit creep data, and a $(1-t)^{3/2}$ power law has been explicitly observed in high-temperature measurements, it is more reasonable to assume a temperature dependence which flattens out at low temperatures in a manner consistent with the scaling of thermodynamic parameters. We thus view the fits of Fig. 3(b) to be physically more realistic even though they incorporate the use of an additional fitting parameter. The values of this fitting parameter were in reasonable agreement with the observed irreversibility line. The product of v_0a can be determined to be on the order of 10^4 cm/sec, which is larger than that observed for grain-aligned Y-1:2:3 samples previously.⁹

Figure 4(a) shows the U_{eff} data of Fig. 3(a) scaled by $H^{0.9}$, where H is measured in T [similar scaling is also possible from the data of Fig. 3(b)]. This figure thus shows that relaxation data between 0.5 and 3.0 T can be placed on a nearly universal $U_{\text{eff}}(J)$ curve after scaling by $H^{0.9}$. This, of course, suggests an $H^{-0.9}$ power-law dependence of the effective activation energy on applied field. At this time we do not attribute any particular significance to the -0.9 power law for the applied field. An H^{-1} dependence has been observed for pinning energies as derived in previous flux-creep studies.¹ It is not inconceivable that details of the pinning mechanism might reveal a slightly modified field dependence in this weak pinning regime. As will be discussed further, a similar field dependence is consistent with measurements of the hysteretically derived current densities. This final field scaling then illustrates that, for a very large body of

data, the effective activation energy can indeed be separated into the product of simple functions of field, temperature, and current density. The $1/H$ dependence of U_{eff} is consistent with that expected for the critical current density (in the absence of flux creep), J_c .

Figure 4(b) shows that, for all fields, $U_{\text{eff}}(J)$ is adequately described by a $\ln(J)$ dependence over 3–4 orders of magnitude in J . It is also possible to fit this data to a power-law dependence in J as suggested by Feigelman *et al.*,²¹ however, fits of this kind require a description with at least two different power-law regimes. It is not inconceivable that other nonlinear functional forms also give adequate fits to $U_{\text{eff}}(J)$.²² The data illustrated in Fig. 4(b) does, however, demonstrate the utility of the logarithmic fits over a wide range of values of M . This explicit functional form is also of particular utility in explaining the exponential temperature dependence of the

current density which will be discussed later. The relaxation data of Fig. 4 thus can be parameterized in terms of the scaling relationship

$$U_{\text{eff}}(J, H) = \frac{U_1 g(T)}{H^n} \ln \left[\frac{J}{J_c} \right], \quad (9)$$

where the exponent n is determined to be ~ 0.9 and the constant U_1 is $\sim 180 k_B$. Extrapolation of the experimentally observed $U_{\text{eff}}(J)$ behavior to $U_{\text{eff}}=0$ allows for the estimation of J_c . Values of $J_c(H)$ exhibit a reasonable field dependence and magnitude but should nonetheless be viewed with some caution in that they involve an extrapolation over approximately an order of magnitude. The implication of these extrapolated values of J_c is that significant relaxation occurs in the time prior to our first magnetization measurement. In fact, nearly an order of magnitude change in J_c occurs between 0 and 360 sec, the time at which our first data point is taken, if the extrapolated J_c is reliable. A fast, short-time relaxation has been observed for grain-oriented Y-1:2:3 (Ref. 23) so that such rapid initial decays are not without precedent. Further, these decays are most prominent near the irreversibility line and thus are not so surprising here given the shallow irreversibility line of this crystal. A J_c value of 3.2×10^5 is determined from this data for the applied field of 1 T, using the Bean model expression, $J = 30M/R$ and ignoring the small correction for the equilibrium magnetization.

Figure 5(a) shows the temperature dependence of the magnetic hysteresis, ΔM (in emu), for the La-Sr-Cu-O sample in applied fields of 0.5, 1.0, 1.5, 2.0, 2.5, 3.0, 3.5, and 4.0 T. The induced current density J can be determined using the Bean model expression $J = 15\Delta M/R$ for a cylinder using the geometric mean sample radius (0.143 cm) and the magnetic hysteresis (in emu/cm³) $\Delta M = M_+ - M_-$ as determined from hysteresis curves and the sample volume (0.02 cm³) which were measured between fields of ± 5 T over a ~ 2 –3 h time period. This slow rate was necessary (at low temperatures) to avoid flux jumps. Even at these slow rates, flux jumps were apparent at temperatures below 5 K and thus our data is truncated at this temperature. The linear dependence of J on ΔM means that the natural logarithm of the current density may be obtained from the data of Fig. 5 by addition of an additive constant (~ 8.6) to the $\ln(\Delta M)$ axis of the figure. We again note that this hysteretically determined current density differs greatly from the critical current density, due to the large relaxations that are possible over the experimental time for measurement of the hysteresis. Notable in this figure is the fit of the J data to an exponential temperature dependence of the form

$$J(T, H) = J_0 \exp \left[\frac{-(T - T^*)}{T_0(H)} \right], \quad (10)$$

where it is experimentally observed that J_0 is a nearly field-independent quantity while T_0 is strongly field dependent and is on the order of ~ 3 K at $H = 1$ T. T^* is on the order of 2 K and represents the temperature at which all but the 0.5-T $J(T, H)$ curves are observed to in-

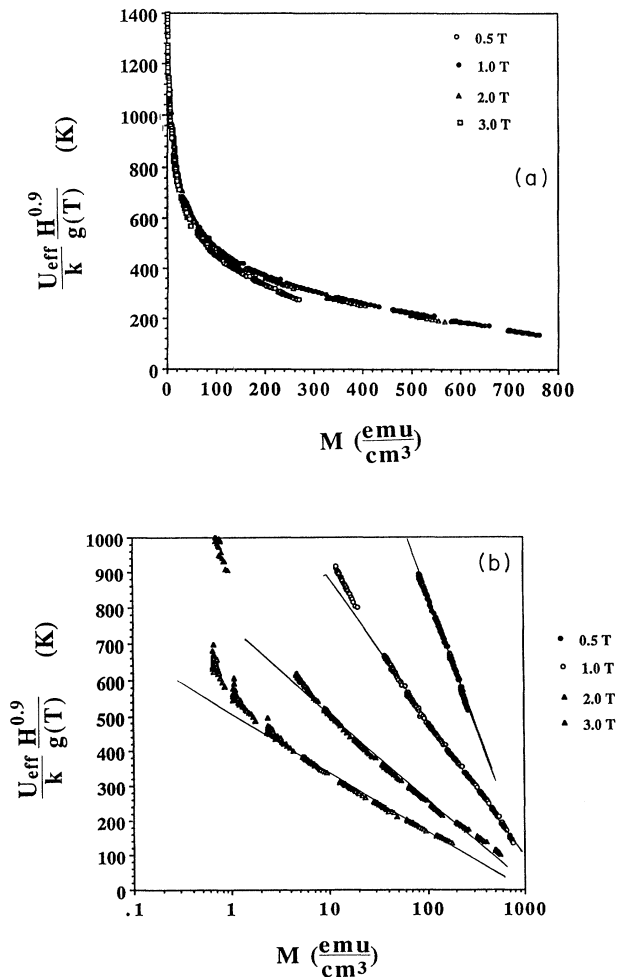


FIG. 4. Fits of $[H^{0.9} U_{\text{eff}}(J)/g(t)]$ vs M for fixed fields of 0.5, 1.0, 2.0, and 3.0 T, respectively, showing an apparent field and temperature scaling of the apparent activation energy for flux creep. Similar results are obtained for scaling by $g(T) = 1 - (T/T^*)^2$.

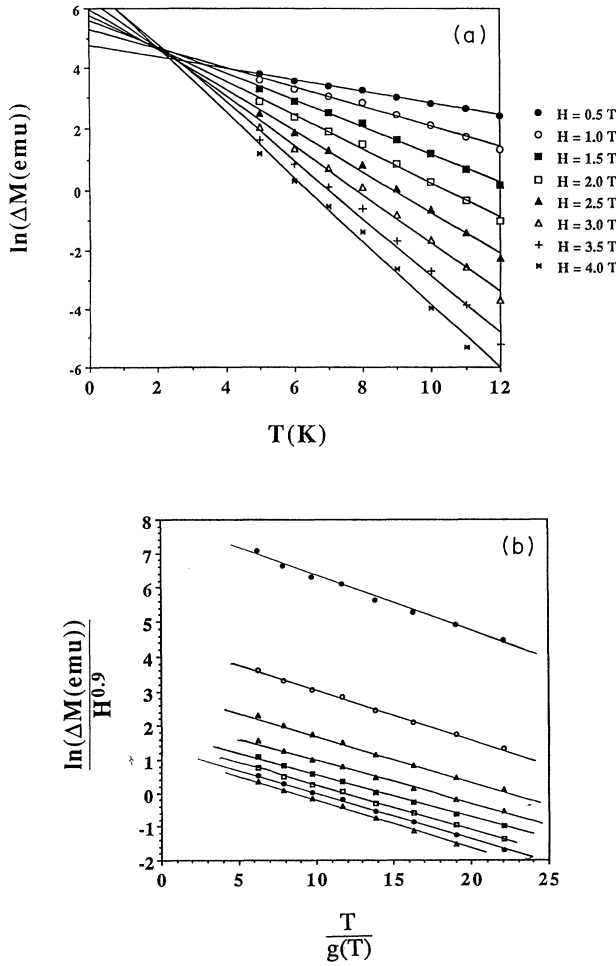


FIG. 5. (a) Natural logarithm of the magnetic hysteresis $\ln(\Delta M)$, ΔM (in emu), from which the hysteretic current density can be determined, as a function of temperature for the La-Sr-Cu-O sample in applied fields of 0.5, 1.0, 1.5, 2.0, 2.5, 3.0, 3.5, and 4.0 T. The magnetic hysteresis is calculated from the differences in the values of M on the increasing and decreasing fields branches of magnetic hysteresis curves. The slopes of these curves give the temperature T_0 which is discussed in the text. (b) $H^{-0.9}\ln(\Delta M)$ vs $T/g(T)$ illustrating similar scaling of T_0 with applied field H as that observed for $U_1(H)$.

intersect. The slightly different temperature dependence of the 0.5-T curve perhaps reflects the fact that, over much of the temperature range explored in this figure, 0.5 T is insufficient to fully penetrate the sample. The parameter J_0 is observed to be $\sim 6 \times 10^5$ A/cm². Values of T_0 at the fields of 0.5, 1.0, 2.0, and 3.0 T were determined to be 5.2, 3.1, 1.9, and 1.4. Notable is the fact that T_0 exhibits nearly the same field dependence as $U_1(H)$.

Figure 5(b) demonstrates that scaling of $\ln(J)$ by $H^{-0.9}$ results in nearly parallel curves as a function of temperature scaled by $g(T)^{-1}$. In the linear ($U \sim J$) flux-creep regime, it is predicted that $J(T)$ should exhibit a linear temperature dependence, i.e.,

$$J(T) = J_c \left[1 - \frac{k_B T}{U_0} \ln \left[\frac{\nu_0}{\nu} \right] \right].$$

This observed exponential behavior of the hysteretically derived current density on temperature, shown in Fig. 5(a) is then inconsistent with the linear flux-creep model. Such a temperature dependence has been observed in Y-1:2:3 single crystals by Senoussi *et al.*²⁴ and others^{25,26} though values of T_0 for Y-1:2:3 are typically seen to be nearly an order of magnitude larger in similar fields. In the latter work this temperature dependence was attributed to micro-Josephson junctions and nonthermally activated response. As we shall see here, this dependence is consistent with the flux-creep model for a nonlinear $[\ln(J)]$ dependence of the effective activation energy for flux creep. In the case of a nonlinear as observed in Figs. 2–4, and realizing that if the frequency is dictated (fixed) by a fixed experimental time, τ , then U_{eff} and J are both related to τ and ν_0 :

$$U_{\text{eff}} = kT \ln(\nu_0 \tau) = - \frac{U_1 g(T)}{H^{0.9}} \ln \left[\frac{J}{J_c} \right]. \quad (11)$$

The first part of expression (11) reflects the Arrhenius law for the approximately fixed frequency of the hysteretic measurement and the second part the experimentally observed $U_{\text{eff}}(J)$ behavior. A consequence of (11) is that the current density measured hysteretically should exhibit an exponential temperature dependence:

$$J \simeq \exp \left[\frac{-T}{T_0} \right], \quad (12)$$

where for fixed frequency experiments T_0 is given empirically from (11) by

$$\frac{T_0}{g(T)} = \frac{U_1 / H^{0.9}}{k \ln(\nu_0 \tau)}, \quad (13)$$

where again τ represents the fixed experimental time scale or, alternatively, the inverse of the fixed frequency. In actuality, there is some small uncertainty in using (13) in that two slightly different values of the experimental time τ are relevant here, one for the M_+ and the other for the M_- points on the hysteresis curve from which the hysteretic current density is calculated. Given the previously derived value of U_1 , it is possible to calculate values of $\ln(\nu_0 \tau)$ for each of these curves. Using the slope of these lines and U_1 a value of ~ 23 is determined for $\ln(\nu_0 \tau)$ which is also seen to be relatively invariant with respect to the applied field. This value of $\ln(\nu_0 \tau)$ is then similar in magnitude to the additive constant determined for the $U_{\text{eff}}(J)$ data. Some of the variance between these two numbers may be attributed to the time scale of the hysteresis experiment.

A most interesting feature of the data illustrated in Fig. 5(a) is the intersection of the hysteretically determined current densities at a temperature $T^* \simeq 2$ K. There are several implications of this observation. First, extrapolation of the J data to $T = 0$ K does not give the value of the critical current density in the absence of

thermal activation. This is apparent because such an extrapolation would yield a physically unreasonable field dependence to this critical current density. It is therefore also apparent that using the linear term in a Taylor series expansion for the exponential dependence of J on temperature ($J \approx \exp(-T/T_0) \approx [1 - (T/T_0)]$) does not lead to an expression equivalent to that predicted for a linear $U(J)$ dependence

$$J(T) = J_c \left[1 - \frac{k_B T}{U_0} \ln \left(\frac{\nu_0}{\nu} \right) \right].$$

Such an expansion might be thought to be a natural extension of the data to lower temperatures if viewed for a single field. However, the crossover of these $J(T)$ curves at ~ 2 K for increasing field is inconsistent with this simple view. These anomalies in the temperature dependence can be taken as an indication that the exponential temperature dependence does not extend to lower temperatures, i.e., that this fit is only valid over a limited temperature range. This again may be seen as consistent with a picture in which the characteristic relaxation kinetics are changing in going from low to high temperatures or equivalently from short to long times. Such a notion is also not inconsistent with the possibility of non-thermally activated response at low temperatures²⁷ ($< \sim 2$ K). Nonetheless, the behavior of the slope of the observed $\ln(J)$ versus T curves is consistent with our picture of relaxation arising from a nonlinear effective potential. The data of Fig. 5(b), which reflect the appropriate field and temperature scaling of the effective activation energies, do not suffer from the crossover of $J(T)$ versus T for different values of the applied field. Instead, the data can be extrapolated to reveal reasonable values for J_c , as well as a reasonable field dependence at 0 K. This observation illustrates the importance of the field and temperature scaling. Summarizing, the critical current density data shown in Fig. 5 is shown to be consistent with the energy and frequency scales derived from the magnetic relaxation data. In particular, the exponential temperature dependence arises naturally from a nonlinear effective flux-creep activation energy.

Another way of independently setting the scale of the attempt frequency is through comparison of measurements of the temperature dependence of the logarithmic magnetic relaxation rate in fixed field, as given by (6) and the temperature dependence of the magnetization at fixed times. Rice *et al.*²⁸ have noted striking similarities between the shape of the temperature-dependent magnetic relaxation rate, $A = dM/[d \ln(t)]$, and the derivative of the magnetization with respect to temperature at fixed time (of ~ 20 min), dM_0/dT , both at small fixed fields ($H \sim 0.1$ T). Their data show that, typically, A and dM_0/dT are of the same order of magnitude. Their analysis indicates that quantitatively different behavior of the relaxation is to be expected at fields greater or less than that required for full penetration. We have similarly determined logarithmic relaxation rates from our magnetization versus time data. Figure 6 shows typical magnetization versus time data for our La-Sr-Cu-O crystal taken over a 2 h period after application of a field of 1 T.

For most of this time interval, the magnetization is quite accurately fit to a $\ln(t)$ dependence. It is clear, however, that at short times and especially at high temperatures this fit is progressively less precise. Values of the logarithmic magnetic relaxation rate are determined from the slope of such magnetization versus $\ln(t)$ plots.

Figure 7 shows a similar comparison to that of Rice *et al.*²⁸ of A and dM_0/dT for our sample at fields of 0.5, 1.0, 2.0, and 3.0 T, respectively. Here M_0 is the fitted value of $M(t)$ at the typical starting time of the relaxation experiments $\tau \sim 360$ sec, though the temperature dependence is relatively insensitive to choices of the fixed time. Notable in this figure is the similarity in the temperature dependence A and dM_0/dT with peaks occurring at similar temperatures, in all cases, though the magnetic relaxation rate is smaller by a factor of ~ 4 than dM_0/dT . Note that, for the data shown in Fig. 7, relaxation data at the fixed fields of 0.5 and 1.0 T are included for temperatures at which these fields are not sufficient to penetrate the sample. This data is similar to that reported in Ref. 24. However, instead of appealing to a specific hysteretic model to explain the details of relationship between A and dM_0/dT we view this similarity in a somewhat different light by appealing again to the rate equation.

Perhaps a more telling comparison of temperature dependences is between that of A and $T g(T)(dM_0/dT) = g(T)[dM_0/d \ln(T)]$ as shown in Fig. 8. This distinction is predicated on the assertion that our observable M or J is a relaxed quantity and therefore determined by the Arrhenius law of expression (1). If we assume no specific form for the relationship between U_{eff} and the applied field and current density, then we can simply write the reduced energy γ :

$$\gamma = \frac{U_{\text{eff}}}{kT} = \ln(\nu_0 t) = F(J), \quad (14)$$

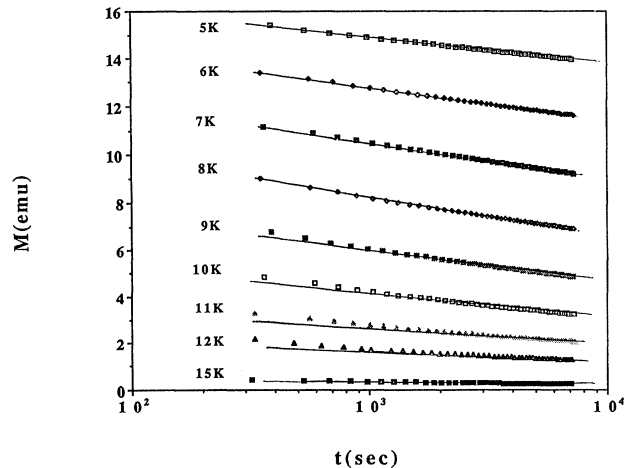


FIG. 6. Comparison of the temperature dependence of the magnetic relaxation data $M(t)$ in an applied field of 1 T from which the logarithmic relation rate $A = dM/[d \ln(t)]$ is derived.

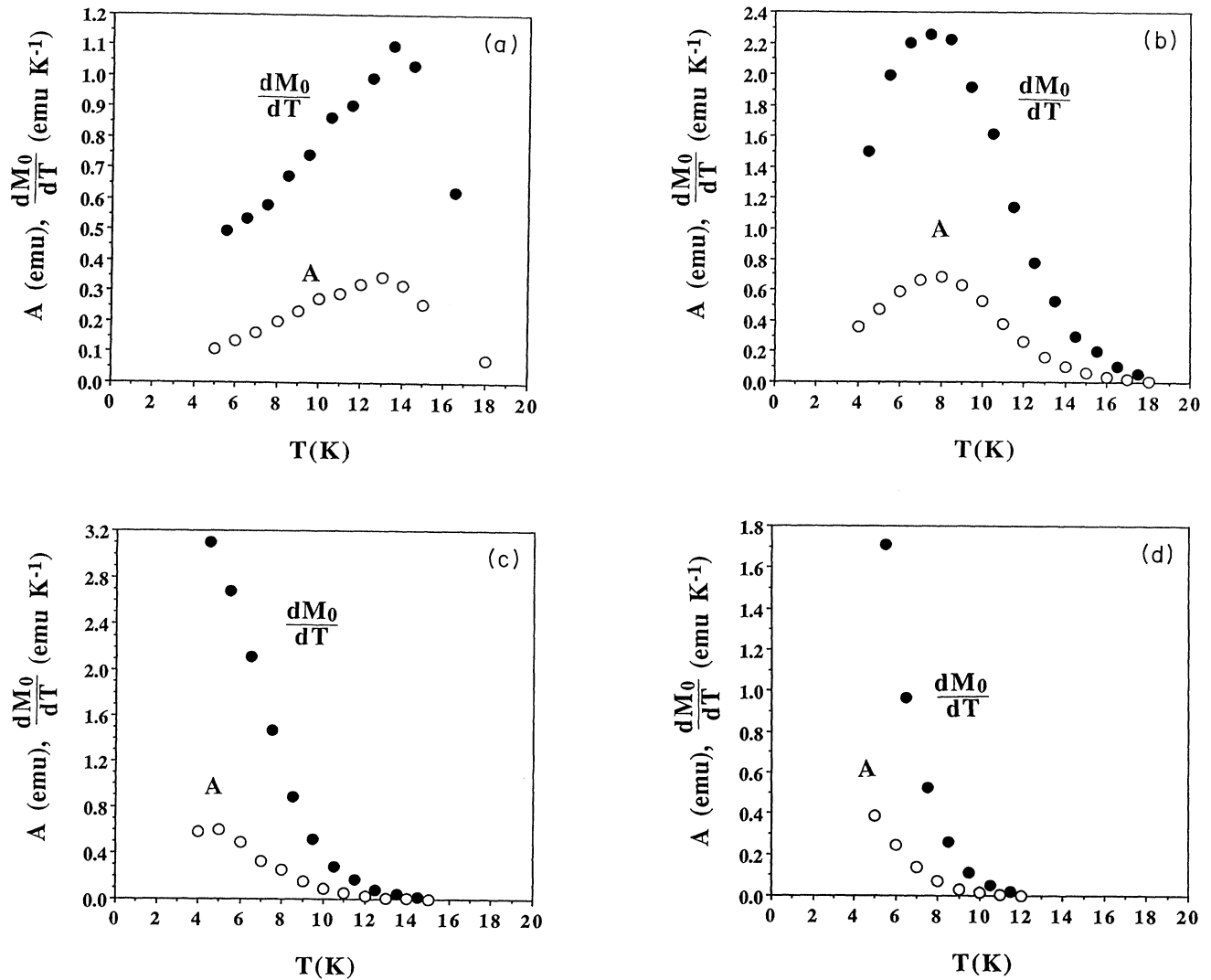


FIG. 7. Comparison of the temperature dependence of the magnetic relaxation rate $A = dM/[d \ln(t)]$ and dM_0/dT for a *c*-axis-oriented La-Sr-Cu-O crystal at fields of (a) 0.5, (b) 1.0, (c) 2.0, and (d) 3.0 T, respectively. M_0 is the fitted value of $M(t)$ at the typical starting time of the relaxation experiments $t = \sim 360$ sec.

where t represents the experimental time, ν_0 is the attempt frequency, and F is an unspecified function of current density at a fixed applied field. The first of these expressions reflects the Arrhenius law for the thermally activated hopping over a barrier. Expression (14) can be differentiated to yield (for fixed fields)

$$d\gamma = -\frac{U_{\text{eff}}}{kT^2} dT + \frac{1}{kT} \left[\frac{\partial U_{\text{eff}}}{\partial J} \right]_H dJ = d \ln(t). \quad (15)$$

We now examine this relationship at fixed temperatures where it can be seen that this expression can be differentiated with respect to $\ln(t)$ and at fixed temperature to yield

$$\left[\frac{\partial M}{\partial \ln(t)} \right]_{T,H} \simeq \left[\frac{\partial J}{\partial \ln(t)} \right]_{T,H} = kT / \left[\frac{\partial U_{\text{eff}}}{\partial J} \right]_H. \quad (16)$$

This is, of course, equivalent to expression (6) described in the Introduction. Similarly, for experiments performed at a fixed time or at fixed frequency, i.e., $t = \tau$, expression (15) can be differentiated with respect to $\ln(T)$ and at this fixed time to yield

$$\left[\frac{\partial M}{\partial \ln(T)} \right]_{\tau,H} \simeq \left[\frac{\partial J}{\partial \ln(T)} \right]_{\tau,H} = U_{\text{eff}} / \left[\frac{\partial U_{\text{eff}}}{\partial J} \right]_H. \quad (17)$$

Comparing (16) and (17), it can be finally seen that $A = dM/[d \ln(t)]$ and $dM_0/[d \ln(T)]$ related by the factor $\ln(\nu_0\tau)$:

$$\left[\frac{\partial M}{\partial \ln(T)} \right]_{\tau} / \left[\frac{\partial M}{\partial \ln(t)} \right]_T = \frac{U_{\text{eff}}}{kT} = \ln(\nu_0\tau). \quad (18)$$

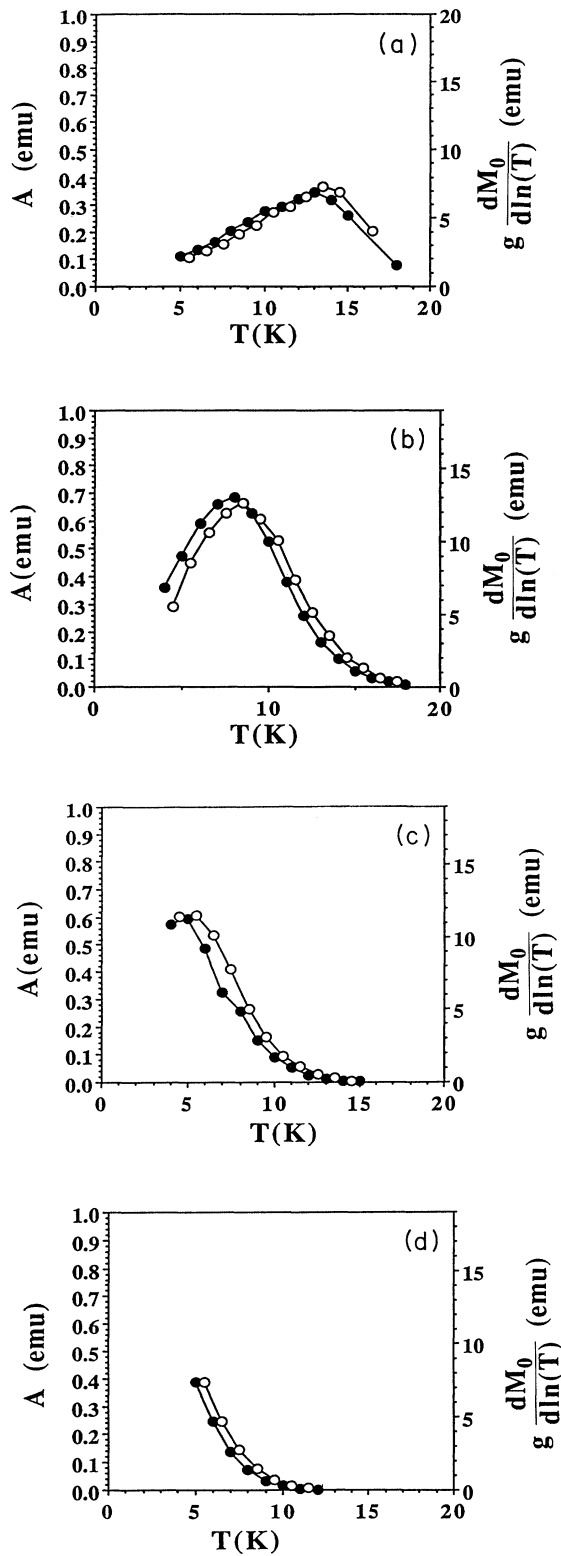


FIG. 8. Comparison of the temperature dependence of the magnetic relaxation rate $A = dM/[d \ln(t)]$ and $g(T)[dM_0/d \ln(T)]$ for a *c*-axis-oriented La-Sr-Cu-O crystal at fields of (a) 0.5, (b) 1.0, (c) 2.0, and (d) 3.0 T, respectively. Note the difference in scale between A and $dM_0/[d \ln(T)]$ at the various fields.

Finally, if we consider the appropriate temperature scaling, $g(T)$ of the apparent activation energy, then we arrive at the relationship

$$g(T) \left[\frac{\partial M}{\partial \ln(T)} \right]_{\tau} / \left[\frac{\partial M}{\partial \ln(t)} \right]_T = U_{\text{eff}} kT = \ln(\nu_0 \tau). \quad (19)$$

Indeed, we have compared the ratio of $dM_0/[d \ln(T)]$ and $A = dM/[d \ln(t)]$ as given by (18) and found values of $\ln(\nu_0 \tau)$ of ~ 40 , ~ 25 , ~ 20 , and ~ 20 for the applied fields of 0.5, 1.0, 2.0, and 3.0 T, respectively. Again these are similar to the values of the constant C found before investigation of the T scaling of U_{eff} . If we consider the temperature scaling, then a comparison of $g(T)[dM_0/d \ln(T)]$ and A is appropriate as shown in Fig. 8. Apparent in Fig. 8 is the fact that, for all fields examined, the temperature dependences of A and $g(T)[dM_0/d \ln(T)]$ are identical to within a scaling parameter of the order of 19 and a shift of temperature of $< \sim 1$ K. Most notable, however, is the relative scale of the two sets of data. Values of $\ln(\nu_0 \tau)$ are inferred which are entirely consistent with those previously arrived at from a consideration of the constant term, C , in the derivation of the nonlinear $U_{\text{eff}}(J)$. These values are nearly independent of the applied field for 0.5, 1.0, 2.0, and 3.0 T as examined here. Given the fact that our procedure for extracting the $U_{\text{eff}}(J)$ behavior from magnetic relaxation measurements involved the addition of a constant which was large in comparison to the typical range of $\ln(dM/dt)$ values examined over the experimental times, it is important to corroborate the scale of this constant. The results of Fig. 5 certainly are in excellent agreement with the previously determined values.

The expression derived from the one-dimensional flux diffusion equation contains a grouping of terms $(H\nu_0 a/2\pi d)$, the natural logarithm of which serves as an additive constant to magnetic relaxation data. In the analysis of the data of the other experiments, the frequency is used in the thermodynamic analysis based on an Arrhenius rate equation. The data scatter from different experiments is such that a precise deconvolution of the hop distance and attempt frequency contributions (and their field dependences) is not possible from the data. However, several meaningful inferences can be obtained from the data. First, there is some disparity in the frequency scales and their temperature dependence for the experiments based on magnetic relaxation and those determined from analysis of the temperature dependence of the hysteretic magnetization currents. This could simply be due to the distinction that the former experiments sample only from the virgin magnetization curve while the latter samples from both the field increasing and field decreasing branches of the hysteresis curves. From the value of the constant, C , and assuming a hop distance of ~ 100 Å, attempt frequencies can be inferred from the data as being $\sim 2 \times 10^{10}$ Hz relatively independent of applied field.

Several points are also worth emphasizing by way of comparison of the experimentally derived energy and frequency parameters for the La-Sr-Cu-O crystal as compared with those of the previously studied grain-aligned

Y-1:2:3 material. In the case of grain-aligned Y-1:2:3, the additive constant C in the $U_{\text{eff}}(J)$ data was 18 for an applied field of 1 T, somewhat smaller than the values reported here. The Y-1:2:3 crystals were also on the order of 10^{-3} cm., as compared with the 10^{-1} cm size of this La-Sr-Cu-O crystal. This implies that the attempt frequency is perhaps several orders of magnitude larger in the La-Sr-Cu-O material than in Y-1:2:3. In general, at similar fields (i.e., $H = 1$ T), the effective activation energy for flux creep in the c -axis-oriented Y-1:2:3 sample is larger than that of a similarly c -axis-oriented La-Sr-Cu-O crystal at equivalent value of the current density.

CONCLUSIONS

In summary, three different sets of experimental conditions, the first relying on magnetic relaxation measurements, the second on magnetic hysteresis, and the third which relies on explicit logarithmic relaxation and the temperature-dependent magnetization all have been shown to reveal similar values of the fundamental attempt frequency for flux hopping and the effective energy scale for flux motion in this material. The behavior of the time and temperature dependence of the magnetization appears to be deeply rooted in a nonlinear $U_{\text{eff}}(J)$ behavior the functional form of which has been characterized for our La-Sr-Cu-O crystal. $U_{\text{eff}}(J)$ has been shown to obey a simple field scaling which is also manifest in the observed temperature dependence of hysteretic magnetization currents. Scaling by a function of reduced temperature resulted in the use of a single additive constant, as

described by the simple diffusion formula, for all fields. A reasonable low-temperature form of this scaling law requires that temperatures be reduced by T_{irr} instead of T_c . The observed exponential dependence of the hysteretically derived current density on temperature can be explained in terms of a nonlinear $U_{\text{eff}}(J)$, specifically one obeying a $\ln(J)$ dependence. The construction of the $U_{\text{eff}}(J)$ curve from magnetic relaxation data requires the addition of a large additive constant to $M(t)$ data and might be viewed as a source of some uncertainty. However, the scale of this parameter has been corroborated through measurements of the magnetic relaxation rates and comparison with the derivative of the static magnetization with respect to the logarithm of temperature. The self-consistency of these experiments is seen to reinforce the validity of our model of the relaxation in this system. By way of comparison, the attempt frequency parameter appears to be much larger in the La-Sr-Cu-O than in the Y-1:2:3 system. Our particular La-Sr-Cu-O crystal exhibited much smaller values of U_{eff} at similar values of J than previously observed in Y-1:2:3.

ACKNOWLEDGMENTS

One of the authors (MEM) would like to gratefully acknowledge the hospitality of Dr. R. Quinn and the Exploratory Research and Development Center at Los Alamos National Laboratory where much of this work was completed.

- ¹Y. Yeshurun and A. P. Malozemoff, *Phys. Rev. Lett.* **60**, 2202 (1988).
- ²C. W. Hagena and R. Griessen, *Phys. Rev. Lett.* **62**, 2856 (1989).
- ³M. E. McHenry, M. P. Maley, E. L. Venturini, and D. L. Grinley, *Phys. Rev. B* **39**, 4784 (1989).
- ⁴H. S. Lessure, S. Simizu, and S. G. Sankar, *Phys. Rev. B* **40**, 5165 (1989).
- ⁵T. T. M. Palstra, B. Batlogg, L. F. Schneemeyer, and J. V. Waszczak, *Phys. Rev. Lett.* **61**, 1662 (1988).
- ⁶M. J. Ferrari, M. Johnson, F. C. Wellstood, J. C. Clarke, P. A. Rosenthal, R. H. Hammond, and M. R. Beasley, *IEEE Trans. Mag.* **25**, 806 (1989).
- ⁷T. K. Worthington, Y. Yeshurun, A. Malozemoff, R. M. Yandrovsky, F. H. Holtzberg, and T. R. Dinger *J. Phys. (Paris)* **C8**, 2093 (1989).
- ⁸M. R. Beasley, R. Labusch, and W. W. Webb, *Phys. Rev.* **181**, 682 (1969).
- ⁹M. P. Maley, J. O. Willis, H. Lessure, and M. E. McHenry, *Phys. Rev. B* **42**, 2639 (1990).
- ¹⁰E. Zeldov, M. M. Amer, G. Koren, A. Gupta, M. W. McElfresh, and R. J. Gambino, *Appl. Phys. Lett.* **56**, 680 (1990).
- ¹¹Y. Xu, M. Suenaga, A. R. Moodenbaugh, and D. O. Welch, *Phys. Rev. B* **40**, 10882 (1989).
- ¹²M. E. McHenry, J. O. Willis, M. P. Maley, J. D. Thompson, J. R. Cost, and D. E. Peterson, *Physica C* **162-164**, 689 (1989).
- ¹³J. Van Den Berg, C. J. Van Der Beek, P. Koorevaar, P. H. Kes, J. A. Mydosh, M. J. V. Menken, and A. A. Menovsky, *Supercond. Sci. Technol.* **1**, 242 (1989).
- ¹⁴I. Tanaka and H. Kojima, *Nature (London)* **337**, 21 (1989).
- ¹⁵A. Migliori, W. M. Visscher, S. Wong, S. E. Brown, I. Tanaka, H. Kojima, and P. B. Allen, *Phys. Rev. Lett.* **64**, 2458 (1990).
- ¹⁶R. B. VanDover, E. M. Gyorgy, L. F. Schneemeyer, J. W. Mitchell, K. V. Rao, R. Puzniak, and J. V. Waszczak, *Nature* **342**, 55 (1989).
- ¹⁷M. Tinkham, *Phys. Rev. Lett.* **61**, 1658 (1988).
- ¹⁸M. V. Feigelman and V. M. Vinokur, *Phys. Rev. B* **41**, 8986 (1990).
- ¹⁹V. M. Vinokur, P. H. Kes, and A.E. Koshelev, *Physica C* **168**, 29 (1990).
- ²⁰T. T. M. Palstra, B. Batlogg, L. F. Schneemeyer, and J. V. Waszczak, *Phys. Rev. B* **43**, 3756 (1991).
- ²¹M. V. Feigelman, V. B. Geshkenbein, A. I. Larkin, and V. M. Vinokur, *Phys. Rev. Lett.* **63**, 2303 (1989).
- ²²A. P. Malozemoff and M. P. A. Fisher, *Phys. Rev. B* **42**, 6784 (1990).
- ²³H. Kupfer, C. Keller, R. Meier-Hirmer, U. Wiech, K. Salama, V. Selvamanickam, S. M. Green, H. L. Luo, and C. Politis, *Phys. Rev. B* **41**, 838 (1990).
- ²⁴S. Senoussi, M. Ousenna, G. Collin, and I. A. Campbell, *Phys. Rev. B* **37**, 9792 (1988).
- ²⁵B. M. Lairson, J. Z. Sun, J. C. Bravman, and T. H. Geballe, *Phys. Rev. B* **42**, 1008 (1990).
- ²⁶M. Naito, A. Matsuda, K. Kitazawa, S. Kambe, I. Tanaka, and H. Kojima, *Phys. Rev. B* **41**, 4823 (1990).
- ²⁷A. Hamzic, L. Fruchter, and I. A. Campbell, *Nature* **345**, 515 (1990).
- ²⁸J. P. Rice, D. M. Ginsberg, M. W. Rabin, K. G. Vandervoort, G. W. Crabtree, and H. Claus, *Phys. Rev. B* **41**, 6532 (1990).